A Unified View of Ethylene Polymerization by d^0 and d^0f^n Transition Metals. 3. Termination of the Growing Polymer Chain

Peter Margl,† Liqun Deng, and Tom Ziegler*

Contribution from the Department of Chemistry, University of Calgary, 2500 University Drive, NW, Calgary, Alberta T2N 1N4, Canada

Received June 8, 1998. Revised Manuscript Received October 23, 1998

Abstract: We present a systematic investigation of chain-termination processes for a number of d^0 $[L]MR^{(0,+,2+)}$ fragments (M = Sc(III), Y(III), La(III), Lu(III), Ti(IV), Zr(IV), Hf(IV), Ce(IV), Th(IV), and V(V); L = $NH\text{-}(CH)_2NH^{2-}$ [1], $N(BH_2)(CH)_2(BH_2)N^{2-}$ [2], $O(CH)_3O^-$ [3], Cp_2^{2-} [4], $NHSi(H_2)C_5H_4^{2-}$ [5], $[(oxo)(O(CH)_3O)]^{3-}$ [6], $(NH_2)_2^{2-}$ [7], $(OH)_2^{2-}$ [8], $(CH_3)_2^{2-}$ [9], $NH(CH_2)_3NH^{2-}$ [10], $O(CH_2)_3O^{2-}$ [11], and DPZ [12]; R = C_2H_5, C_3H_7) involved in ethylene polymerization. Our calculations show that β-hydrogen transfer to the monomer is the dominant chain-termination mechanism under the usual experimental conditions. β-Hydrogen elimination (i.e., hydrogen transfer to the metal) can only compete in the limit of very small monomer concentrations or if monomer complexation is otherwise disfavored. The activation barrier for β-hydrogen transfer to the monomer is only weakly dependent on the character of the metal center and the auxiliary ligand. The thermodynamic driving force as well as the kinetic barrier of β-hydrogen elimination is highly dependent on the metal, but only weakly dependent on the auxiliary ligand set. We lay out rules to affect BHE and BHT barriers, and, by comparing the termination activation barriers with data on ethylene insertion barriers, we provide guidelines along which successful ethylene polymerization catalysts may be designed.

Introduction

Due to many recent experimental advances in the design of homogeneous Ziegler−Natta-type catalysts, the family of single-site olefin polymerization catalysts has proven much larger than one would have expected a few years ago. It extends across the periodic table, involving not only early transition metals but also late ones such as Fe(II), Co(II), Ni(II), and Pd(II).[1−5] Much experimental effort is, however, still devoted to d^0-transition-metal systems, with a focus on the group 4 metals Ti, Zr, and Hf,[6−23] accompanied by substantial contributions by the theoretical chemistry community, of which only a select few can be shown in our limited bibliography.[24−41]

* To whom correspondence should be addressed. Tel.: (403) 220-5368. Fax: (403) 289-9488. E-mail: ziegler@acs.ucalgary.ca or ziegler@zinc.chem.ucalgary.ca.

† Present address: Eastman Chemical Company, P.O. Box 1972, Kingsport, TN 37662-5150.

(1) Killian, C. M.; Tempel, D. J.; Johnson, L. K.; Brookhart, M. *J. Am. Chem. Soc.* **1996**, *118*, 11664.

(2) Rix, F. C.; Brookhart, M.; White, P. S. *J. Am. Chem. Soc.* **1996**, *118*, 4746.

(3) Brookhart, M.; DeSimone, J. M.; Tanner, M. J. *Macromolecules* **1995**, *28*, 5378.

(4) Small, B. L.; Brookhart, M.; Bennett, A. M. A. *J. Am. Chem. Soc.* **1998**, *120*, 4049.

(5) Britovsek, G. J. P.; Gibson, V. C.; Kimberley, B. S.; Maddox, P. J.; McTavish, S. J.; Solan, G. A.; White, A. J. P.; Williams, D. J. *Chem. Commun.* **1998**, 849.

(6) Scollard, J. D.; McConville, D. H. *J. Am. Chem. Soc.* **1996**, *118*, 10008.

(7) Scollard, J. D.; McConville, D. H.; Payne, N. C.; Vittal, J. J. *Macromolecules* **1996**, *29*, 5241.

(8) Shah, S. A. A.; Dorn, H.; Voigt, A.; Roesky, H.; Parisini, E.; Schmidt, H.-G.; Noltemeyer, M. *Organometallics* **1996**, *15*, 3176−3181.

(9) Fokken, S.; Spaniol, T. P.; Kang, H.-C.; Massa, W.; Okuda, J. *Organometallics* **1996**, *15*, 5069−5072.

(10) van der Linden, A.; Schaverien, C. J.; Meijboom, N.; Ganter, C.; Orpen, A. G. *J. Am. Chem. Soc.* **1995**, *117*, 3008−3021.

(11) Warren, T. H.; Schrock, R. R.; Davis, W. M. *Organometallics* **1996**, *15*, 562−569.

(12) Brand, H.; Capriotti, J. A.; Arnold, J. *Organometallics* **1994**, *13*, 4469.

(13) Tjaden, E. B.; Swenson, D. C.; Jordan, R. F.; Petersen, J. L. *Organometallics* **1995**, *14*, 371−386.

(14) Horton, A. D.; de With, J.; van der Linden, A. J.; van de Weg, H. *Organometallics* **1996**, *15*, 2672−2674.

(15) Fuhrmann, H.; Brenner, S.; Arndt, P.; Kempe, R. *Inorg. Chem.* **1996**, *35*, 6742−6745.

(16) Cozzi, P. G.; Gallo, E.; Floriani, C.; Chiesi-Villa, A.; Rizzoli, C. *Organometallics* **1995**, *14*, 4994−4996.

(17) Cloke, F. G. N.; Geldbach, T. J.; Hitchcock, P. B.; Love, J. B. *J. Organomet. Chem.* **1996**, *506*, 343−345.

(18) Uhrhammer, R.; Black, D. G.; Gandner, T. G.; Olsen, J. D.; Jordan, R. F. *J. Am. Chem. Soc.* **1993**, *115*, 8493−8494.

(19) Long, D. P.; Bianconi, P. A. *J. Am. Chem. Soc.* **1996**, *118*, 12453.

(20) Aoyagi, K.; Gantzel, P. K.; Kalai, K.; Tilley, T. D. *Organometallics* **1996**, *15*, 923−927.

(21) Jia, L.; Yang, X.; Stern, C.; Marks, T. J. *Organometallics* **1994**, *13*, 3755.

(22) Murphy, V. J.; Turner, H. *Organometallics* **1997**, *16*, 2495−2497.

(23) Antonelli, D. M.; Leins, A.; Stryker, J. M. *Organometallics* **1997**, *16*, 2500−2502.

(24) Janiak, C. *J. Organomet. Chem.* **1993**, *452*, 63.

(25) Jolly, C. A.; Marynick, D. S. *J. Am. Chem. Soc.* **1989**, *111*, 7968.

(26) Castonguay, L. A.; Rappe, A. K. *J. Am. Chem. Soc.* **1992**, *114*, 5832.

(27) Prosenc, M.-H.; Brintzinger, H.-H. *Organometallics* **1997**, *16*, 3889.

(28) Kawamura-Kuribayashi, H.; Koga, N.; Morokuma, K. *J. Am. Chem. Soc.* **1992**, *114*, 2359.

(29) Kawamura-Kuribayashi, H.; Koga, N.; Morokuma, K. *J. Am. Chem. Soc.* **1992**, *114*, 8687.

(30) Bierwagen, E. B.; Bercaw, J. E.; Goddard, W. A., III. *J. Am. Chem. Soc.* **1994**, *116*, 1481−1489.

(31) Gleiter, R.; Hyla-Kryspin, I.; Niu, S.; Erker, G. *Organometallics* **1993**, *12*, 3828.

(32) Mohr, R.; Berke, H.; Erker, G. *Helv. Chim. Acta* **1993**, *76*, 1389.

(33) Froese, R. D. J.; Musaev, D. G.; Matsubara, T.; Morokuma, K. *J. Am. Chem. Soc.* **1997**, *119*, 7190.

(34) Weiss, H.; Ehrig, C.; Ahlrichs, R. *J. Am. Chem. Soc.* **1994**, *116*, 4919.

(35) Yoshida, T.; Koga, N.; Morokuma, K. *Organometallics* **1995**, *14*, 746.

(36) Margl, P.; Deng, L.; Ziegler, T. *J. Am. Chem. Soc.* **1998**, *120*, 5517−5525.

(37) Margl, P.; Deng, L.; Ziegler, T. *Organometallics* **1998**, *17*, 933.

10.1021/ja981995c CCC: $18.00
Published on Web 12/19/1998

Scheme 1

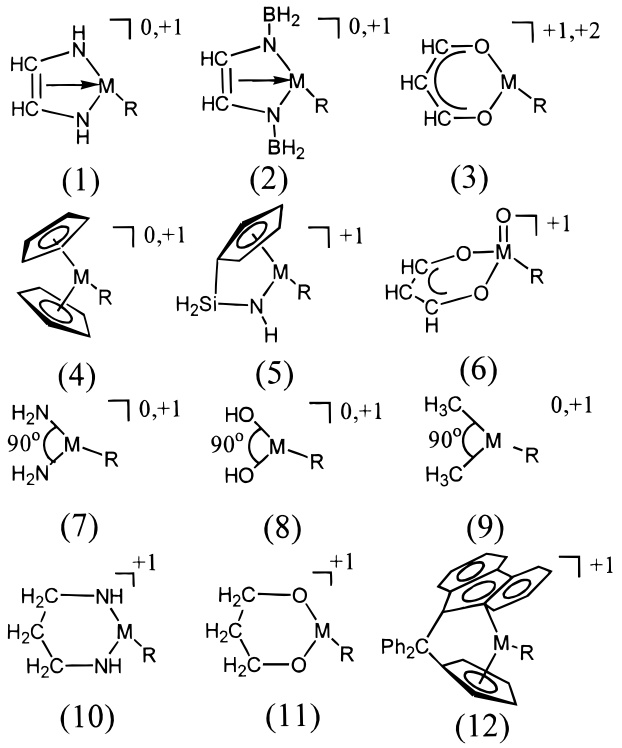

As part of a project to set up a theoretical framework for single-site polymerization, the present series of papers attempts to develop a unified description of d^0-metal-catalyzed Ziegler−Natta olefin polymerization. The prequels of the present study[36,37] described the energetics of the metal−ligand framework, of ethylene uptake, and of chain propagation. In the present paper, we complete our work by presenting the chain-termination energetics of a sample of 45 catalysts of the general composition $[L]MR^{(0,+,2+)}$ (M = Sc(III), Y(III), La(III), Lu(III), Ti(IV), Zr(IV), Hf(IV), Ce(IV), Th(IV), and V(V); L = $NH(CH)_2NH^{2-}$ [1], $N(BH_2)(CH)_2(BH_2)N^{2-}$ [2], $O(CH)_3O^-$ [3], Cp_2^{2-} [4], $NHSi(H_2)C_5H_4^{2-}$ [5], $[(oxo)(O(CH)_3O)]^{3-}$ [6], $(NH_2)_2^{2-}$ [7], $(OH)_2^{2-}$ [8], $(CH_3)_2^{2-}$ [9], $NH(CH_2)_3NH^{2-}$ [10], $O(CH_2)_3O^{2-}$ [11], and DPZ [12]; R = C_2H_5, C_3H_7 (Scheme 1). We will, furthermore, give an assessment of catalyst activity for the catalysts investigated here, using the present data set as well as data on olefin uptake and chain propagation that has been calculated previously. This enables us to set up a set of rules on which the rational design of a new catalyst can be based. In this approach, we neglect factors that are related to a counterion or a solvent. As shown in Scheme 2, the chain-propagation process for Ziegler-type catalysts is initiated by olefin uptake (a) followed by an insertion reaction (b) between the metal−polymer bond and the incoming olefin. The often-dominant competing process is transfer of a polymer β-hydrogen atom to the approaching olefin (c), leading to termination of the chain and regrowth of a new chain, after the terminated chain has been ejected (d). In the present study, we describe step (c). Polymer molecular weight can be decreased not only by β-hydrogen transfer but also, as shown in Scheme 2, by hydrogen elimination from the agostic precursor (e). In the present paper, we do not, in detail, consider the ejection processes that must follow steps c and e and which are necessary to complete the termination reaction. Energetic aspects of the first-order ethylene-uptake/-ejection process have been considered in part 1 of this study[37] and will not be further analyzed here, as trends derived there can be supposed to be identical for the systems investigated here. Second-order displacements of the vinyl-terminated chain, however, can be a rather complex process, as one has to consider, explicitly, the role of entropic factors. A detailed investigation of these effects exceeds the scope of the present paper.

As in the predecessors to this study, we do not explicitly consider steric hindrance deriving from large substituents, since it is our aim to outline the influence of the metal and the first coordination sphere on olefin complexation and insertion energetics. Exceptions to this are sterically bulky ligands that form an irreducible entity such as in $(Cp)_2$. Larger ligands, such as DPZ, will be considered in places where it seems expedient. They are, however, not the direct object of our study.

For our calculations along the β-hydrogen transfer (BHT) pathway, we use an ethyl group as a model for the growing polymer chain, a measure which has been rationalized in previous publications[38,39] and which represents an optimum choice for balancing physical accuracy and computing resources. For calculations on the β-hydrogen elimination (BHE) pathway, however, we use a propyl group to model the growing chain, because an ethyl group gives an unnaturally high barrier for the elimination as well as a higher endothermicity.[38,39]

Computational Details

Stationary points on the potential energy surface were calculated with the program ADF, developed by Baerends et al.,[42,43] using the numerical integration scheme developed by te Velde et al.[44] The frozen-core approximation was employed throughout. The electronic configurations of the molecular systems were described by a triple-ζ Slater-type basis set on metal atoms and by a double-ζ quality basis on nonmetal atoms. The exact makeup of the basis sets used is described in parts 1 and 2 of this study.[36,37] A set of auxiliary[45] s, p, d, f, and g STO functions, centered on all nuclei, was used in order to fit the molecular density and present Coulomb and exchange potentials accurately in each SCF cycle. Energy differences were calculated by augmenting the local exchange-correlation potential by Vosko et al.[46] with Becke's nonlocal exchange corrections[47] and Perdew's nonlocal correlation correction[48,49] (BP86). Geometries were optimized including nonlocal corrections. First-order scalar relativistic corrections were added to the total energy for all systems containing 3d and 4d metal atoms, since a perturbative relativistic approach is sufficient for those as shown by Deng et al.[50] On all systems containing lanthanide, actinide, or 5d metal atoms, quasi-relativistic calculations[51,52] were carried out. In view of the fact that all systems investigated in this work show a large HOMO−LUMO gap, a spin-restricted formalism was used for all calculations for compounds with an even number of electrons. No symmetry constraints were used. Transition states were located by minimizing all degrees of freedom, while keeping a specific internal

(38) Woo, T. K.; Margl, P.; Ziegler, T.; Blöchl, P. E. *Organometallics* **1997**, *16*, 3454.
(39) Woo, T.; Margl, P. M.; Lohrenz, J. C. W.; Blöchl, P. E.; Ziegler, T. *J. Am. Chem. Soc.* **1996**, *118*, 13021.
(40) Woo, T. K.; Fan, L.; Ziegler, T. *Organometallics* **1994**, *13*, 432.
(41) Woo, T. K.; Fan, L.; Ziegler, T. *Organometallics* **1994**, *13*, 2252.
(42) Baerends, E. J.; Ellis, D. E.; Ros, P. *Chem. Phys.* **1973**, *2*, 41.
(43) Baerends, E. J.; Ros, P. *Chem. Phys.* **1973**, *2*, 52.
(44) te Velde, G.; Baerends, E. J. *J. Comput. Chem.* **1992**, *99*, 84.
(45) Krijn, J.; Baerends, E. J. *Fit Functions in the HFS Method*; Department of Theoretical Chemistry, Free University: Amsterdam, The Netherlands, 1984.
(46) Vosko, S. H.; Wilk, L.; Nusair, M. *Can. J. Phys.* **1980**, *58*, 1200.
(47) Becke, A. *Phys. Rev. A*: At., Mol., Opt. Phys. **1988**, *38*, 3098.
(48) Perdew, J. P. *Phys. Rev. B*: Condens. Matter **1986**, *34*, 7406.
(49) Perdew, J. P. *Phys. Rev. B*: Condens. Matter **1986**, *33*, 8822−8824.
(50) Deng, L.; Ziegler, T.; Woo, T. K.; Margl, P.; Fan, L. *Organometallics* **1998**, *17*, 3240−3253.
(51) Ziegler, T.; Tschinke, V.; Baerends, E. J.; Snijders, J. G.; Ravenek, W. *J. Phys. Chem.* **1989**, *93*, 3050.
(52) Li, J.; Schreckenbach, G.; Ziegler, T. *Inorg. Chem.* **1995**, *34*, 3245−3252.

Scheme 2

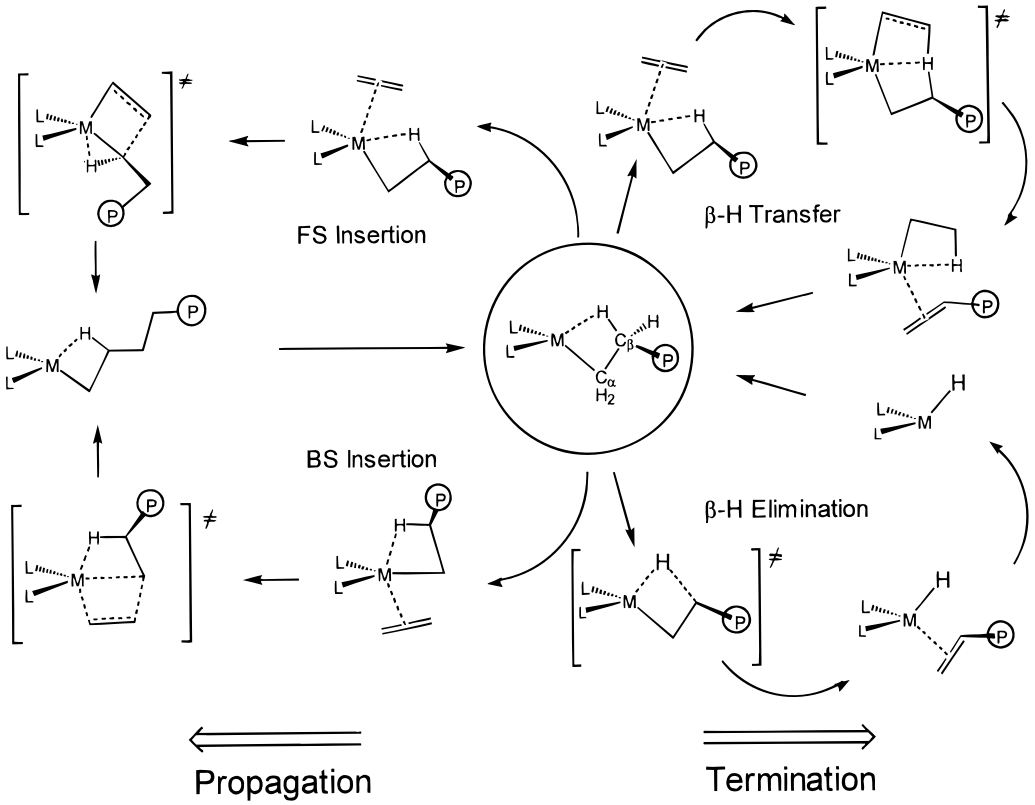

coordinate fixed. The internal coordinate in this case was the distance between the β-carbon and β-hydrogen bond that is being broken during BHE or BHT, respectively. Previous experience with [10]Ti/Zr/Hf,[50] as well as with [4]Zr,[56] shows that the transition states obtained by this transit method are identical to transition states located by eigenvector following.

In a number of previous papers, transition metal−ligand dissociation energetics obtained on the level of theory outlined above have been shown to be correct within 5 kcal/mol of the experimental result, usually overestimated in terms of absolute size.[53,54] Activation energies have been shown to be generally lower by 2−4 kcal/mol than the experimental estimate.[53,54] In a recent benchmark computational study, Jensen and Børve[55] have shown that the BP86 functional gives results in excellent agreement with the best wave-function-based methods available today for the class of reactions investigated here.

Results and Discussion

The results of our DFT calculations are summarized in Table 1. In the following we will discuss the details of the β-hydrogen transfer and elimination mechanisms.

(1) The *β*-Hydrogen Transfer Mechanism. As shown in Scheme 2, β-hydrogen transfer proceeds from the β-agostic front side (FS) π-complex through a pseudo-mirror symmetric transition state, where the transferring hydrogen atom is at roughly equal distance from the β-carbon of the alkyl chain and the syn carbon of the ethylene unit. Previous investigations have made it seem likely that the BHT mechanism is the most favored of all chain-termination mechanisms, in the absence of a counterion and without the inclusion of solvent effects.[38,39] Here, we embark on a systematic study of the BHT mechanism that will allow us to either fortify or discard this tentative notion. For our computational studies of the BHT mechanism, we model the growing alkyl chain with an ethyl group. This level of abstraction has been justified on several occasions in the literature, and we will not further discuss this issue here.

A glance at Table 1 shows that the BHT barriers are quite low on an absolute scale and that there is little dependence of the barrier height on metal and ligand. This notion is spelled out by Figure 1, where the BHT barriers for all systems investigated here are plotted as a function of the metal center. However, there are systematic trends present: (a) group-3 and group-4 d^0 BHT barriers are of comparable magnitude, with the group-3 barriers being slightly higher. Non-d^0 group-4 BHT barriers are much higher. (b) For both the group-3 and group-4 triads, we notice a slow increase of the BHT barrier upon moving to heavier metals. This increase is more pronounced for the group-3 metals. (c) Steric congestion around the metal center tends to push BHT barriers up, as seen for [4]Sc and [6]V. In the following we will rationalize this behavior in terms of bond contributions to the total energy.

(1a) Energetic Decomposition of BHT Transition States [L]M··C_2H_4··H··$C_2H_4$$^{n+}$ (n = 0−2). To localize the origin of the BHT activation barrier, we decompose the process $[L]MC_2H_5(C_2H_4)^{n+} \rightarrow [L]MC_2H_4\cdot\cdot H\cdot\cdot C_2H_4^{n+}$ into five fictitious stages according to Scheme 3, writing the total activation barrier as

$$\Delta E_{\mathrm{BHT}}^{\ddagger} = \Delta E_{\pi} + \Delta E_{\mathrm{M-C}} = \Delta E_{\mathrm{def}} + \Delta E_{\mathrm{M-H}} + \Delta E_{\pi-\mathrm{TS}} \quad (1)$$

By calculating this decomposition for a series of metals with a fixed auxiliary ligand, we can localize the origin of the rising trend of the BHT barrier as a function of the metal center. Table 2 shows the decomposition data we have calculated for group-3 and group-4 d^0 metals coordinated by ligand [7].

(53) Margl, P.; Ziegler, T. *Organometallics* **1996**, *15*, 5519.
(54) Margl, P. M.; Ziegler, T. *J. Am. Chem. Soc.* **1996**, *118*, 7337.
(55) Jensen, V.; Borve, K. *J. Comput. Chem.* **1998**, *19*, 947.
(56) (a) Lohrenz, J. C. W.; Woo, T. K.; Ziegler, T. *J. Am. Chem. Soc.* **1995**, *117*, 12793. (b) Note that Table 1, ref 54 incorrectly cites the insertion TS energies for [4]Zr. The correct values are FS as follows: −20 (−15); BS, −16 (replacing −23 and −27). The insertion barriers are cited *correctly*.

Table 1. Barriers for the Chain Termination Processes "β-Hydrogen Transfer to the Monomer" (BHT) and "β-Hydride Elimination" (BHE) for All Compounds Investigated

		termination barrier		ΔE^m			termination barrier		ΔE^m
metal	ligand	BHT[a]	BHE[b]	BHE[b]	metal	ligand	BHT[a]	BHE[b]	BHE[b]
Sc[III]	[1]-exo	39	63	64	Ti[IV]	[1]-exo	31	82	73
	[2]-exo[l]	40	54	44		[2]-exo[l]	32		4
	[3]	36	75	62		[3]	27	77	55
	[4][h]	58	110	110		[4][h]	35	141	141
	[7]	42	75	67		[5][d]	32	61	54
	[8]	41	70	62		[7]	30	59	59
	[9]	37	77	77		[8]	30	67	64
Y[III]	[1]-exo	41	69	59		[9]	14	78	67
	[7]	46	70	55		[10]-endo[c,g]	33	82	82
	[8]	44	72	55		[11]-exo[g]	22	70	48
	[9]	41	76	76	Zr[IV]	[1]-exo	35	73	53
La[III]	[1]-exo	47	76	70		[3]	32	66	31
	[7]	51	84	73		[4]	30[e]	45[j]	39[j]
	[8]	48	84	74		[7]	35	68	38
	[9]	53	90	87		[8]	36	69	49
Lu[III]	[1]-exo	38	72	44		[9]	33	71	56
Ti[III]	[7][f]	77	44	22		[10]-endo[c,g]	29	62	49
Ti[III]	Cl_4[f,i]	82	110	108		[11]-exo[g]	29		
						[12][k]		41	25
					Hf[IV]	[1]-exo	38	83	40
						[4]	36	43	30
						[7]	40	100	47
						[8]	40	102	41
						[9]	40	111	57
						[10]-endo[c,g]	34	72	42
					Th(IV)	[1]-exo	49	82	68
					V(V)	[6]	89	91	91

[a] In kJ/mol. Relative to the π-complex $[L]MC_2H_5(C_2H_4)^{n+}$. [b] In kJ/mol. Relative to the most stable conformation of the precursor $[L]MC_3H_7^{n+}$. [c] Results taken from Deng et al.[50] [d] Results taken from Woo et al.[38] [e] Result taken from Lohrenz et al.[56] [f] Not a d^0 system. [g] Propyl group used to model the growing polymer chain for BHT and BHE mechanisms. [h] The BHE product is unstable and reverts to the agostic precursor. Energy to form $[L]MH^{n+}$ + propene is given instead for the total reaction energy. [i] Result for the heterogeneous Ti[III] catalyst by Cavallo et al.[62], on the same level of theory as this work. [j] Results for BHE from Prosenc et al.[27], on the same level of theory as this work. [k] from QM/MM calculations.[61] [l] BHE data unreliable due to incipient B−H activation of the auxiliary ligand. [m] Reaction energy for BHE.

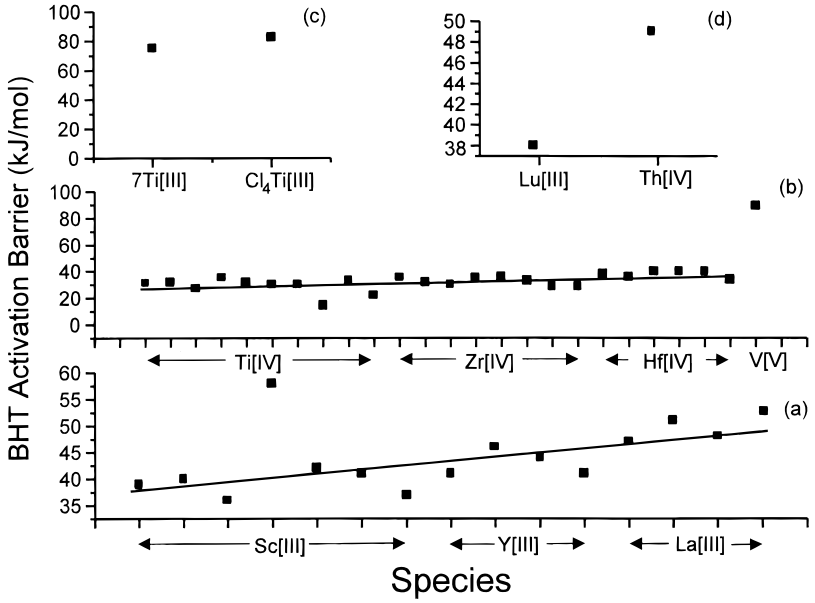

Figure 1. β-Hydrogen transfer (BHT) activation barriers for all complexes listed in Table 1, in kJ/mol. Catalysts are grouped according to the central metal atom. Ligands appear in the same sequence as in Table 1, from left to right. (a) Group 3 metal catalysts. (b) Group 4 metal catalysts and 6V[V]. (c) d^1 systems. (d) Lu[III] and Th[IV].

Table 2 shows that the most dominant contribution to the trend in the BHT barrier is the change in the metal−carbon and metal−hydride bond strengths. For the group-3 triad, we see the M−C bond strength becomes stronger as we go down a triad, but this change is overcompensated for by the M−H bond, which is weakened even more. For the group-4 triad, the M−C bond becomes weaker from Ti to Zr, but regains some strength for Hf. The M−H bond, on the other hand, becomes weaker throughout, leading to an increase in the barrier height. The lower barrier of the charged group-4 complexes can be explained considering the bonding arrangement around the metal center during the BHT transition state: the transition state is crowded around the metal, the close contact allowing for optimal stabilization of negative-ligand charge by the positively charged

Scheme 3

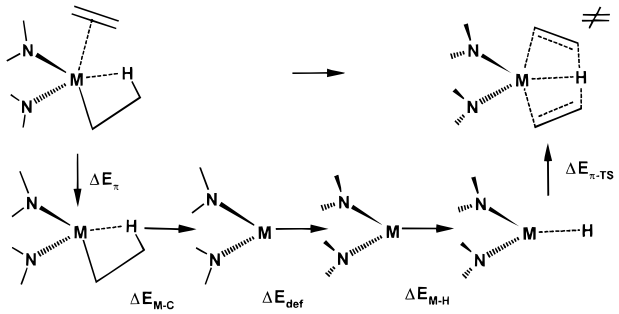

Table 2. Decomposition of the BHT Activation Barriers of Compounds of the Type [7] $MC_2H_5(C_2H_4)^{n+}$ [a]

	$\Delta\Delta E_\pi$	$\Delta\Delta E_{M-C}$	$\Delta\Delta E_{def}$	$\Delta\Delta E_{M-H}$	$\Delta\Delta E_{\pi-TS}$	$\Delta\Delta E_{rel}$	$\Delta\Delta E_{BHT}^{\ddagger}$
Sc	0	0	0	0	0	0	0
Y	0	−35	−2	43	0	0	6
La	−16	−90	−6	107	15	−	10
Ti	48	750	−2	−628	−178	0	−10
Zr	47	675	−10	−552	−163	−2	−5
Hf	41	690	−4	−543	−185	−	−1

[a] Bond strengths refer to heterolytic cleavage (Scheme 3). All values in kJ/mol, with respect to [7]$ScC_2H_5(C_2H_4)^{n+}$.

metal. Thus, the π system in the TS can be bound more effectively to the metal, lowering the barrier. *We can therefore conclude that the increase in the barrier when going from lighter metals to heavier metals is caused by a stronger weakening of the M−H bond as compared to that of the M−C bond in the precursor. The lowering of the BHT activation barrier on going from group-3 to group-4 metals can be explained by a better stabilization of the olefinic ligand system through interaction with the charged metal. This is not possible for group-3 metals, which, therefore, exhibit a higher barrier.* An alternative—but equally consistent—way of expressing the same fact can be found considering the behavior of metal−ligand bond strength as a function of the trigonal-planar−trigonal-pyramidal conversion outlined in part 1 of this study.[37] It was found that trigonal planar arrangement (such as found during the BHT transition state, where the H atom is in the plane with the ML_2 ligand framework) is more favorable for group-3 than for group-4 metals and for 3d metals than for 5d metals. Conversely, the trigonal-pyramidal state (such as found in the π complex) is more favorable for group-4 metals and for heavy members of the triad. From this trend of relative stabilization of ground state compared to transition state it follows that the BHT barrier is lowest for 3d metals and highest for 5d metals, and it is higher for group-4 metals than for group-3 metals.

(1b) BHT Activation Barriers for Sterically Encumbered Systems. Visual examination of the transition-state structures (provided in the Supporting Information) shows remarkable similarity among all structures, regardless of the metal and the ligand. The general motif is the pseudo-C_{2v} symmetric hydridic structure that has been found on many occasions in previous work.[38,56] The sole exceptions to this standard geometry are the sterically extremely congested systems, whose geometry is dictated by the steric makeup of the active site. Although the selection of our ligand set was aimed at creating small and computationally tractable systems, there are some examples in which the ligand system creates strong steric congestion around the metal center. Systems of small ions such as [4]Sc, [4]Ti, and [6]V, especially, exhibit significant steric blockage around the active site, as already discussed in part 1 of this study. For those, we observe in Table 1 a tendency toward high BHT activation barriers. The origin of this trend is that the BHT transition state needs a lot of free coordination space on the metal to be able to bind two ethylene units plus one hydride. The greater the congestion around the metal center, the less space is available for the formation of the BHT transition state. If no hydridic bond can be formed at all at the BHT transition state (as in the case of [6]V), the BHT barrier becomes prohibitively high (Table 1 and Figure 1). A pictorial representation of this situation can be found in Scheme 4. *We can conclude this section by stating that it seems possible to tailor a high BHT barrier by imposing steric constraints on the active site. A small metal ion (Sc, Ti, or V) or a bulky ligand (e.g., ligand [4] or a tridentate ligand) is more likely to have a high BHT barrier.*

Scheme 4

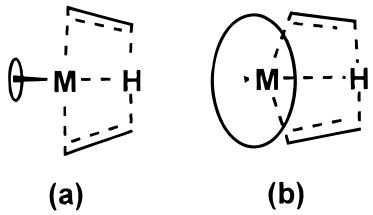

(1c) Ejection of the Vinyl-Terminated Chain after BHT. To lead to a true termination event, instead of only a chain branching event, the terminated chain must be ejected from the active site. This can be done in two ways: first, the vinyl-terminated chain can be ejected by a first-order mechanism, leaving behind the agostic precursor. It is thus the exact reverse of the ethylene uptake reaction discussed in part 1 of this study,[37] except for the polymer chain dangling from the unsaturated chain terminus. We will here assume that the energetics computed for this step in part 1 of this study are qualitatively unchanged. *Thus, first-order ejection of the terminated chain will be more difficult for charged complexes than for uncharged complexes, and for sterically open complexes it will be more difficult than for sterically encumbered complexes. For sterically open, charged complexes such as [10]Zr or [11]Zr (which have a positive ejection energy of ~100 kJ/mol), it will be virtually impossible to eject a terminated chain by a first-order mechanism. On the other hand, for uncharged and/or sterically hindered complexes, such as [4]Sc and [4]Ti, for which ethylene uptake is virtually thermoneutral, every BHT event will, in fact, lead to ejection of the terminated chain.*

Second-order ejection, whereby an incoming monomer smoothly replaces the terminated chain, is supposed to be more favorable, as the energy loss accompanying the dissociation of the π complex is compensated by energy gain from forming another π complex. We are not aware of any published data on second-order substitutions of this sort. A computational investigation of this would by far exceed the focus of the present paper. We can, however, with reasonable certainty state that under high monomer pressure, second-order substitution of the terminated chain will become increasingly facile. Preliminary calculations[57] suggest that it might, in fact, be thermoneutral even for charged complexes.

(2) The β-Hydrogen Elimination Mechanism. The BHE mechanism, as shown in Scheme 2, has been found to be slower for bis-Cp type complexes of Ti and Zr[27,38] in previous studies. However, it has not been proven that this is necessarily the case for all d^0-type catalysts and for ligands other than derivatives of Cp. BHE proceeds from the β-agostic precursor, through a transition state that exhibits a substantially elongated $C_\beta-H_\beta$ bond, to an olefin hydrido product. Previous studies on this

(57) Moscardi, G.; Deng, L.; Woo, T. Private communication, 1997.

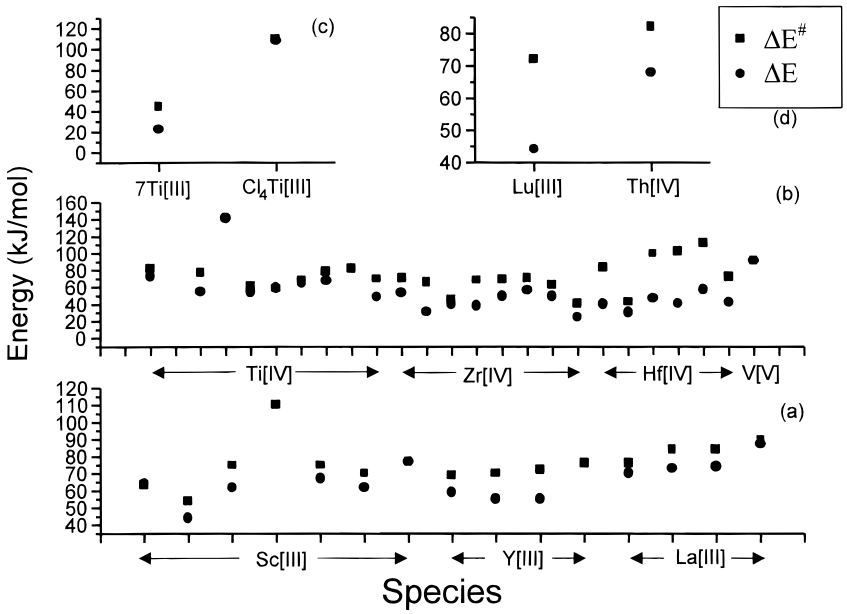

Figure 2. Reaction energies (circles) and activation barriers (squares) for β-hydride elimination (BHE) for all complexes listed in Table 1. See also Figure 1.

reaction[27,38] make it seem necessary to use a propyl group as a model for the growing chain, because both activation barrier and thermodynamic barrier for the process are overestimated if a shorter chain is used.

(2a) The Agostic Precursors for BHE [L]$MC_3H_7^{n+}$ (n = 0, 1, 2). The properties of the agostic precursors to BHE ([L]$MC_3H_7^{n+}$) are not significantly different from the agostic precursor compounds [L]$MC_2H_5^{n+}$ that have been discussed in part 1 of this study. We will therefore not discuss their differences here. Instead, we refer to the Supporting Information for more details.

(2b) The BHE Transition States [L]$MC_3H_6H^{n+}$ (n = 0−2). Table 1 and Figure 2 show that the height of the BHE barrier is not a straightforward function of the metal. In contrast to the BHT barrier, there is no clearly visible trend either as a function of the metal or of the ligand. A comparison of BHE and BHT barriers shows that the BHT barrier is always lower. *It is a general finding of the present study that the BHE elementary reaction is always slower than the BHT elementary reaction if the precursors (the FS π complex for BHT and the β-agostic alkyl for BHE) are present in equal concentrations.*

However, it might be desirable in some cases to keep the monomer concentration low during polymerization, and in such cases it is important to be aware of the factors that govern the speed of BHE. Detailed analysis of the BHE activation barriers shows that the barrier heights are determined by a multitude of mutually compensating factors. We will confine ourselves here to a discussion of the most dominant factors and neglect all others for simplicity of discussion. Visual examination of Table 1 shows the following: (a) For group 3 metals, the BHE barriers remain virtually constant for Sc and Y (except for [4]Sc, see note h), but show a slight rise toward La. (b) For the group 4 metals, the Zr BHE barriers seem lowest on average, with Hf having clearly the highest barriers of all d^0 systems. (c) Steric congestion around the metal center seems to very strongly influence the BHE barriers. Especially, we observe that the systems [4]Zr and [12]Zr, which are both Cp derivatives with some amount of steric hindrance, have relatively low barriers in absolute terms. The barriers observed for these two compounds are about 20 kJ/mol lower than those for sterically undemanding ligands. Also, the bis-Cp systems [4]Ti and [4]-Sc show no stable hydrido olefin complex. For them, the dissociation asymptote (>100 kJ/mol) is the elimination barrier. This is significantly higher than the barrier observed for sterically unhindered systems of Ti and Sc.

A weak metal−olefin bond in the BHE transition state (for La) and, additionally, a weak metal−hydride bond (for Hf) primarily cause the higher barriers that are observed for La and Hf under points a and b. This weak metal−olefin binding is a characteristic feature of 5d d^0 metal atoms and has been discussed in Part 1 of this study in the context of π complex formation.[37] The weak metal−hydride binding in the BHE transition state for Hf can be explained by appreciating the fact that, in the BHE transition state, the hydride is forced to be coplanar with the [L]M ligand plane. We have shown in part 1 of this study[37] that coplanarity is energetically extremely unfavorable for Hf. These two influences, namely weak olefin binding and/or weak hydride binding, are responsible for the higher BHE barriers for La and Hf.

The influence of steric congestion mentioned in point c can obviously go in two opposite directions, depending on the metal ion. For the Zr and Hf species, we find that steric congestion reduces the barrier somewhat ([7]Zr, 68; [4]Zr, 45; [12]Zr, 41 or [7]Hf, 100; [4]Hf, 43). In these cases, the lowering of the barrier can be explained by a destabilization of the educt state (which has a bulky propyl group bound tightly to the metal) relative to the product state (which only has a less demanding hydride bound to the metal). A similar observation has already been made by Prosenc et al.[27]

Why is the situation so obviously different for the small-metal ions, which show exactly the opposite effect? Here it is useful to consider the π-complexation energetics outlined in part 1 of this study. Therein, we have shown that the energy of olefin complexation for sterically congested ligands is a near-linear function of the accessible surface area on the metal. For [4]Ti and [4]Sc, which are both rather small metal ions with small accessible surface areas, we have shown that ethylene only gains marginal stabilization by coordinating to the metal ([4]$TiC_2H_5^+$, −8 kJ/mol; [4]ScC_2H_5, 0 kJ/mol). For an even larger propyl group, it is reasonable to assume that this situation would be enforced and that the stabilization the complex can gain by replacing the M−C bond with an M−H bond plus an M−olefin

π bond is too small. Therefore, the sterically extremely congested species do not form a stable hydrido olefin complex. *We can conclude this section by stating that the BHE barrier can be tuned in two ways: First, one might choose a metal that exhibits, on average, the desired barrier height (for instance choosing La and Hf if one desires a high barrier). Second, the BHE barrier reacts very sensitively to steric bulk around the metal site. For larger metal ions, it seems that the barrier can be lowered somewhat by increasing the steric bulk. For very-small-metal ions, it seems that adding steric bulk can increase the barrier, since the π-complexation stabilization energy of the transition state vanishes for extreme steric congestion. This degree of freedom can, however, not be manipulated without detailed knowledge of the potential surface.*

(2c) The BHE Products [L]M(C_3H_6)(H)$^{n+}$ ($n = 0-2$). In Table 1 and Figure 2 we provide the reaction energies for BHE. They determine the thermodynamic stability of the elimination product and, together with the BHE barrier, also the kinetic stability of the olefin hydride complex, which is an issue if one is interested in chain isomerization. An overly large thermodynamic stability can act as a sink that withdraws population from the propagation cycle, if the insertion barrier is low enough to permit frequent formation of the BHE product. A very large kinetic stability, on the other hand, will lead to a highly isomerized product. We will not deal here with the dihydrogen-allyl formation that is likely to occur starting from the BHE product, as recently described by a number of authors.[58-61] Visual examination of Table 1 and Figure 2 reveals that the BHE product stability follows roughly the same trends as the BHE barrier. *Typically, the total energy of the BHE product is roughly 10−20 kJ/mol lower than the BHE transition state. The sole exceptions to this rule are sterically open complexes of Hf, for which the energy of the BHE product is 50 kJ/mol smaller than the BHE transition state.*

Analysis of our results reveals that the factors that govern the thermodynamic stability of the BHE products are identical to those determining the BHE activation barriers, which is not surprising, as transition states and products are geometrically very close. *The means of manipulating the stability of the BHE product are therefore identical to those we can use to manipulate the stability of the BHE transition state.* However, the sterically open complexes of Hf constitute an exception. Our analysis shows that this is caused by a large gain in M−H bonding on going from the BHE transition state to the BHE product. The primary difference between the BHE product and BHE transition state is that the hydride is forced to be coplanar with the [L]M plane in the BHE transition state, but can adopt its most favored configuration (perpendicular to the [L]M plane) in the BHE product. This gives rise to a strong stabilization of the BHE product over the BHE transition state for Hf. For the other metals, this preference of perpendicular vs coplanar is less pronounced, and therefore the elimination product is less stabilized over the transition state. *We can conclude this section by stating that the trends observed for the BHE products are identical to those observed for the educts, with the exception of Hf, which tends to have kinetically as well as thermodynamically very stable elimination products.*

(2d) Ejection of the Vinyl-Terminated Chain after BHE. The conclusions drawn above, namely that BHT is a more effective chain termination mechanism than BHE, are enforced by considering the difficulty of completing the termination event by ejection of the terminated chain. The typical first-order ejection energy for an olefin from the active [L]M$C_2H_5^{n+}$ center after a BHT event is between 0 and 110 kJ/mol, as shown in part 1 of this study[37] for the case of ethylene. On the other hand, our calculations on [4]Sc and [4]Ti indicate that the ejection energy for an olefin after a BHE event is substantially larger, the dissociation asymptote lying above the agostic precursor by as much as 140 kJ/mol. This comes from the fact that the metal hydride that is formed after BHE binds an olefin much more strongly than the metal alkyl formed after BHT, which is sterically more congested and thus does not bind olefin as effectively as the hydride. *In light of this fact, it is likely that even **if** rare BHE events take place, they will more likely end in chain isomerization than in chain ejection and, thus, termination. However, steric congestion around the metal center and/or low monomer concentration can shift the balance from BHT to BHE.*

(3) Comparison of Chain Propagation vs Chain Termination. Knowing that the BHT is always the dominant chain termination step under sufficient monomer concentration, we are now in a position to assess the effectiveness of different catalysts by comparing their insertion barriers as presented in part 2 of this study[36] with the termination barriers. Since both FS insertion (usually the rate-limiting elementary reaction for insertion) and BHT originate from the same structure (namely the FS ethylene π complex), we can directly compare the two barriers without any need to account for different populations of the precursors. In Figure 3, we juxtapose FS insertion barriers and BHT barriers.

Mere visual examination of Figure 3 shows that, depending on the metal center, there is a different relation between the FS propagation barrier and the BHT termination barrier. *For group-3 metals, there is good separation (20−30 kJ/mol) between the FS insertion barrier and the BHT barrier, so that group-3 metal catalysts have a high intrinsic aptitude toward chain propagation. For group-4 cations, the situation is much less favorable toward propagation. The separation between insertion and termination barriers is much smaller and tends to reverse its sign on going from Ti to Hf. This is caused by the strong rise of the FS insertion barrier upon moving down the triad, as discussed in part 2 of this study. The BHT barrier, on the other hand, shows much less dependence on the metal center, so that the lines formed by FS insertion barriers and BHT barriers intersect in the middle of the triad. It is therefore necessary to find an auxiliary ligand that minimizes the insertion barrier in order to get a polymerization catalyst, because the intrinsic aptitude of the metal toward insertion is not enough to ensure this.* We have, in part 2 of this study, outlined methods by which ligands can be chosen that maximize the aptitude toward insertion. For Lu and Th, insertion barriers are well separated from the termination barriers, and we propose here that actinides in general will be fairly good polymerization catalysts, even without auxiliary ligand modification.

A totally different case is presented by the non d^0 systems. Figure 3 shows that for a sterically open Ti system ([7]Ti) the insertion barrier is higher than the termination barrier. We have shown in part 2 of this study that group-4 non-d^0 systems generally exhibit higher insertion barriers than d^0 systems. Therefore, it will be more difficult to design a workable catalyst based on a metal ion with d electrons than one based on a d^0 system. Recently, however, Cavallo and co-workers[62] have shown that strong steric modifications of the auxiliary ligand

(58) Margl, P. M.; Woo, T. K.; Blöchl, P. E.; Ziegler, T. *J. Am. Chem. Soc.* **1998**, *120*, 2174−2175.

(59) Resconi, L. Private communication, 1998.

(60) Richardson, D. E.; Alameddin, G. A.; Ryan, M. F.; Hayes, T.; Eyler, J. R.; Siedle, A. R. *J. Am. Chem. Soc.* **1996**, *118*, 11244.

(61) Margl, P. M.; Woo, T. K.; Ziegler, T. *Organometallics* **1998**, in press.

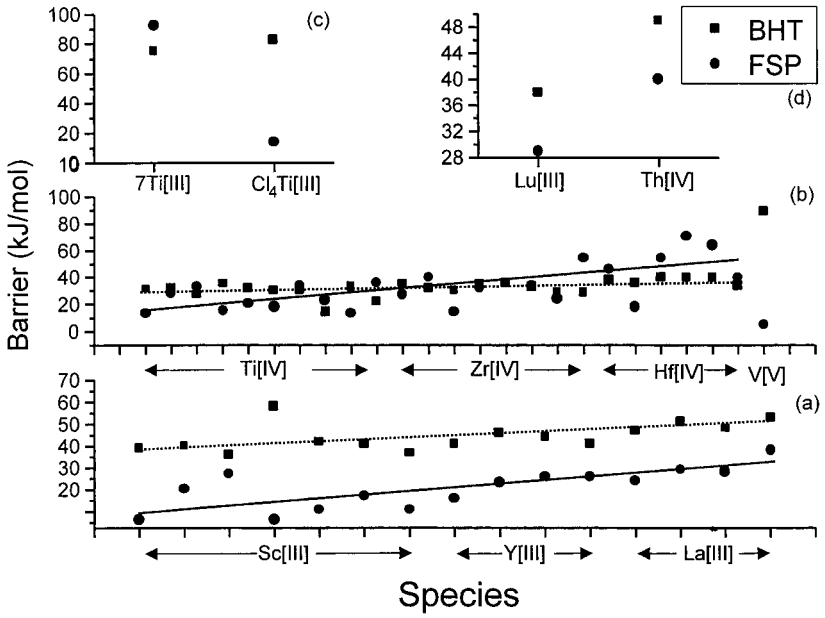

Figure 3. Juxtaposition of front−side insertion (=propagation) barriers (circles) and BHT (=termination) barriers (squares) for all complexes listed in Table 1. Propagation barriers are taken from Part 2 of this study. See also Figure 1.

can greatly reduce the insertion barrier (see Figure 3) and increase the BHT barrier, which is in agreement with our findings. Part c of Figure 3 shows that upon going from a sterically open system ([7]Ti) to a sterically very bulky system (Cl_4Ti), the order of insertion/termination barriers is reversed. We have already alluded to this fact pertaining to insertion in part 2 of this study, and we are now in a position to generalize this to the ratio of insertion to termination. *Steric encumbrance as imposed by bulky auxiliary ligands is an efficient method to lower insertion barriers and simultaneously increase BHT termination barriers for early transition metal d^0 as well as non-d^0 catalysts.* The addition of steric bulk has the effect of increasing the energy of the π complex relative to the insertion transition state (see part 2 of this study[36]), thus lowering the insertion barrier. On the other hand, steric bulk tends to raise the energy of the BHT transition state by the same amount or more than the energy of the π complex, so that the BHT barrier remains constant or is raised, while the insertion barrier is lowered. A good example of this is the living system by McConville et al.,[6,7] which employs selective steric pressure on the π complex and the BHT transition state to achieve high polymer molecular weights.

(3a) Application−Zirconocene vs Hafnocene Derivatives. In this section, we illustrate how our data can be used to rationalize experimental facts. We focus on the prominent case of zircono and hafnocene derivatives, for which experimental molecular weight and activity data is available.[63] Although the experimental data was obtained for racemic ethylene(bisindenyl)M (M = Zr, Hf), and we have investigated only the generic biscyclopentadienyl systems, a limited and cautious comparison is warranted.

Heiland and Kaminsky[63] state that a hafnocene-analogue catalyst (racemic $Et(Ind)_2HfCl_2$) produces polyethylene with molecular weights up to 10 times higher than an analogous zirconocene catalyst does, while at the same time, the hafnocene is more active. From Figure 3 it follows that hafnium catalysts *on average* produce lower molecular weight polymers than zirconium catalysts and that hafnium catalysts *on average* are less active than zirconium ones. However, careful examination of our data (tabulated in parts 1−3 of the present series) shows that the metallocene family—belonging to the sterically more encumbered catalysts—constitutes a notable exception to this rule. In fact, our work (parts 1−3) predicts that a hafnocene catalyst will produce a higher molecular weight polymer while at the same time being more active than a zirconocene catalyst, for the following reasons:

(1) According to our calculations published in part 2 of this work, hafnocene has an insertion barrier (for our purposes, this is equivalent to the propagation barrier) of 18 kJ/mol, which is very similar to the insertion barrier for zirconocene (22 kJ/mol—obtained for a geometry obtained at the same nonlocal level[56] of theory used in the present study for hafnocene). Therefore, hafnocene should insert faster than zirconocene, judging from the relative insertion-barrier heights.

(2) β-Hydrogen transfer is the dominant chain-termination process for ethylene polymerization with both hafno- and zirconocenes in the high-pressure limit. Judging from the speed of chain termination predicted by our calculations in the present work (Table 1), it appears that hafnocene will terminate at a lower rate (barrier: 36 kJ/mol), through the β-hydrogen transfer (BHT) termination channel, than zirconocene (barrier: 30 kJ/mol). At room temperature, this results in an intrinsic termination frequency for the zirconocene that is approximately 10 times faster than that for the hafnocene. Given an otherwise almost equal propagation speed (slightly favoring the hafnocene), our predictions state that under kinetic control hafnocene will produce a polymer with 10 times the molecular weight of zirconocene, and thus our predictions are in perfect agreement with experimental results. In fact, the agreement is so quantitative that it seems fortuitous, considering that we are comparing cyclopentadienyl ligands (theory) to indenyl ligands (experiment).

For the low-pressure limit, we can make a third, synergetic, argument. According to part 1 of this study, hafnocene has a higher olefin sticking probability (FS: −63/BS: −63 kJ/mol) than zirconocene (FS: −37/BS: −44 kJ/mol), where BS means back-side insertion, so that the population of the FS π complex is roughly 35 000 times larger for hafnocene than for zir-

(62) Cavallo, L.; Guerra, G.; Corradini, P. *J. Am. Chem. Soc.* **1998**, *120*, 2428.

(63) Heiland, K.; Kaminsky, W. *Makromol. Chem.* **1992**, *193*, 601.

conocene. This, in turn, means that β-hydrogen elimination (BHE) termination will be disfavored in hafnocene as compared to in zirconocene, while at the same time, insertion will be faster for hafnocene because it has a higher population of the precursor for insertion (the olefin$-\pi$ complex).

Although our comparison is necessarily limited as a result of space requirements, we have shown that our work gives a rather complete set of theoretical parameters that can be used to explain experimental findings and also to predict properties of yet-untested catalyst systems.

Concluding Remarks

The present work represents the conclusion of a trilogy that is aimed at providing an overview of homogeneous Ziegler−Natta polymerization by d^0-transition-metal ions based on density-functional-theory calculations. We have calculated the properties of a large sample of potential catalysts and supplemented our data set with data from the literature. Our data set includes compounds of the type $[L]MR^{(0,1+,2+)}$ (M = Sc(III), Y(III), La(III), Lu(III), Ti(IV), Zr(IV), Hf(IV), Ce(IV), Th(IV), and V(V); L = $NH(CH)_2NH^{2-}$ [1], $N(BH_2)(CH)_2(BH_2)N^{2-}$ [2], $O(CH)_3O^-$ [3], Cp_2^{2-} [4], $NHSi(H_2)C_5H_4^{2-}$ [5], $[(oxo)(O(CH)_3O)]^{3-}$ [6], $(NH_2)_2^{2-}$ [7], $(OH)_2^{2-}$ [8], $(CH_3)_2^{2-}$ [9], $NH(CH_2)_3NH^{2-}$[10], $O(CH_2)_3O^{2-}$ [11], and DPZ [12]; R = C_2H_5, C_3H_7). In the present paper, we have provided the kinetics and thermodynamics of β-hydrogen transfer (BHT) and β-hydrogen elimination (BHE) processes, which are the most important chain termination processes known from the literature. We find the following: (a) BHT is the dominant chain-termination mechanism under the usual experimental conditions of high monomer partial pressure. BHE (i.e., hydrogen transfer to the metal) can only compete in the limit of very small monomer concentrations or if the formation of a π complex is otherwise (for instance, sterically) disfavored. (b) The activation barrier for BHT is only weakly dependent on the character of the metal center. However, adding sterically bulky ligands can drastically increase it. (c) The BHE barrier, which is always higher than the BHT barrier, can be tuned in two ways: first, one might choose a first- or second-row metal if one desires a low BHE barrier or a third-row metal to effect the opposite. Second, since the BHE barrier reacts very sensitively to steric bulk around the metal site, one might use the auxiliary ligand as a means of tuning. For larger metal ions, it seems that the barrier can be somewhat lowered by increasing the steric bulk. For very small metal ions, it seems that adding steric bulk can increase the barrier, since the π-complexation stabilization energy of the transition state vanishes for extreme steric congestion. This degree of freedom, however, cannot be manipulated without detailed knowledge of the potential surface. (d) The means for affecting the stability of the BHE products are identical to those observed for affecting that of the educts. (e) The BHE products (the olefin−hydride complexes) are usually 20−30 kJ/mol more stable than the BHE transition states, except for Hf, which tends to have kinetically as well as thermodynamically very stable elimination products (50 kJ/mol below the energy of the BHE transition state). (f) By comparing termination and insertion barriers (the latter have been calculated in part 2 of this study), we have outlined general trends that determine the polymer molecular weight produced. For group-3 metals, there is good separation (20−30 kJ/mol) between the FS insertion barrier and the BHT barrier, so that group-3-metal catalysts have a high intrinsic aptitude toward chain propagation. For group-4 cations, the situation is much less favorable for propagation. The separation between insertion and termination barriers is much smaller and tends to reverse its sign upon going from Ti to Hf. The BHT barrier, on the other hand, shows much less dependence on the metal center, so that the lines formed by FS insertion barriers and BHT barriers intersect in the middle of the triad. It is therefore necessary to find an auxiliary ligand that minimizes the insertion barrier in order to get a polymerization catalyst, because the intrinsic aptitude of the metal toward insertion is not enough to ensure that it will happen. We find, however, that any intrinsic trend imposed by the metal ion can be countered by choosing an appropriate auxiliary ligand. Steric encumbrance as imposed by bulky auxiliary ligands is an efficient method for lowering insertion barriers and simultaneously increasing BHT termination barriers for early-transition-metal d^0 as well as non-d^0 catalysts.

Acknowledgment. This work has been supported by the National Sciences and Engineering Research Council of Canada (NSERC), as well as by the donors of the Petroleum Research Fund, administered by the American Chemical Society (ACS-PRF No 31205-AC3). P.M. acknowledges fruitful discussions with T. K. Woo and R. Schmid.

Supporting Information Available: A listing of Cartesian coordinates for BHT and BHE precursors, transition states, and reaction products (60 pages, print/PDF). See any current masthead page for ordering information and Web access instructions.

JA981995C